Inorg. Chem. **2009**, *48*, 1551−1558

Formation of a Partially Oxidized Gold Compound by Electrolytic Oxidation of the Solvoluminescent Gold(I) Trimer, $Au_3(MeN{=}COMe)_3$

Krzysztof Winkler,[†,*] Monika Wysocka-Żołopa,[†] Katarzyna Rećko,[‡] Ludwik Dobrzyński,[‡] Jess C. Vickery,[§] and Alan L. Balch[§,*]

Institute of Chemistry, University of Bialystok, 15-424 Bialystok, Poland, Institute of Physics, University of Bialystok, 15-399 Bialystok, Poland, and Department of Chemistry, University of California, Davis, California 95616, USA

Received October 8, 2008

The trinuclear complex, $Au_3(MeN{=}COMe)_3$, which displays a number of remarkable properties including solvoluminescence, has been found to undergo electrochemical oxidation with the deposition of long, thin needles on the electrode surface. The electro-deposition process has been studied by cyclic voltammetry, chronoamperometry, and quartz crystal microbalance techniques. The composition of the electrically conducting needles has been determined to be $[Au_3(MeN{=}COMe)_3](ClO_4)_{0.34}$ by two complementary methods. The related complex $Au_3(PhCH_2N{=}COMe)_3$ underwent oxidation at a significantly more positive potential and did not produce a deposit on the electrode surface.

Introduction

The colorless gold(I) trimer, $Au_3(MeN{=}COMe)_3$ whose structure is shown in Chart 1,[1] displays some remarkable luminescent properties. Upon irradiation of a crystalline sample of the complex with near-UV light, a yellow emission is readily observed visually for seconds after irradiation stops.[2,3] The decay is multiexponential and shows a long lifetime component of 31 s. When a liquid such as chloroform or dichloromethane is dropped onto previously irradiated and still glowing crystals of $Au_3(MeN{=}COMe)_3$, a bright burst of yellow light is produced. Because the visually estimated intensity of this emission is greatest for those liquids that are good solvents for $Au_3(MeN{=}COMe)_3$, the phenomenon has been called solvoluminescence.

$Au_3(MeN{=}COMe)_3$ has been crystallized in three polymorphic forms: colorless needles of a hexagonal form,[2] colorless blocks of a monoclinic polymorph, and colorless blocks of a triclinic form.[4] These forms differ in the ways in which the trimeric molecules interact with one another as shown in Chart 2. In this chart, the trinuclear complexes are represented by triangles with the gold atoms at the apexes and solid lines representing the aurophilic interactions between gold(I) centers within a molecule. The aurophilic interactions between molecules are shown as dashed lines, and the bridging ligands are not shown. The aurophilic interactions seen in the solid-state structures of these and many other two-coordinate Au(I) complexes are weakly attractive with bond energies of ca. 7−11 kcal/mol, that is similar to the energies of hydrogen bonds.[5−7] For two-coordinate gold(I) complexes, these weak aurophilic interac-

Chart 1. Trinuclear Gold(I) Complexes

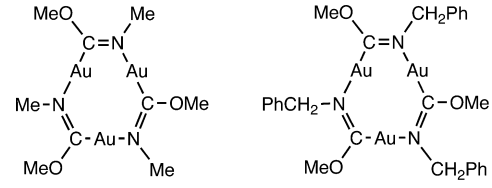

$Au_3(MeN{=}COMe)_3$ $Au_3(PhCH_2N{=}COMe)_3$

* To whom correspondence should be addressed. E-mail: winkler@uwb.edu.pl (K.W.), albalch@ucdavis.edu (A.L.B.). Fax: (530) 752-2820.
† Institute of Chemistry, University of Bialystok.
‡ Institute of Physics, University of Bialystok.
§ Department of Chemistry, University of California, Davis.

(1) Parks, J. E.; Balch, A. L. *J. Organomet. Chem.* **1974**, *71*, 453.
(2) Vickery, J. C.; Olmstead, M. M.; Fung, E. Y.; Balch, A. L. *Angew. Chem., Int. Ed. Engl.* **1997**, *36*, 1179.
(3) Fung, E. Y.; Olmstead, M. M.; Vickery, J. C.; Balch, A. L. *Coord. Chem. Rev.* **1998**, *171*, 151.
(4) White-Morris, R. L.; Olmstead, M. M.; Attar, S.; Balch, A. L. *Inorg. Chem.* **2005**, *44*, 5021.
(5) Schmidbaur, H.; Graf, W.; Müller, G. *Angew. Chem., Int. Ed. Engl.* **1988**, *27*, 417.
(6) Harwell, D. E.; Mortimer, M. D.; Knobler, C. B.; Anet, F. A. L.; Hawthorne, M. F. *J. Am. Chem. Soc.* **1996**, *118*, 2679.
(7) Codina, A.; Fernández, E. J.; Jones, P. G.; Laguna, A.; López-de-Luzuriaga, J. M.; Monge, M.; Olmos, M. E.; Pérez, J.; Rodríguez, M. A. *J. Am. Chem. Soc.* **2002**, *124*, 678.

10.1021/ic801922a CCC: $40.75
Published on Web 01/16/2009

Chart 2. Intramolecular Au···Au Interactions in the Polymorphs of $Au_3(MeN{=}COMe)_3$

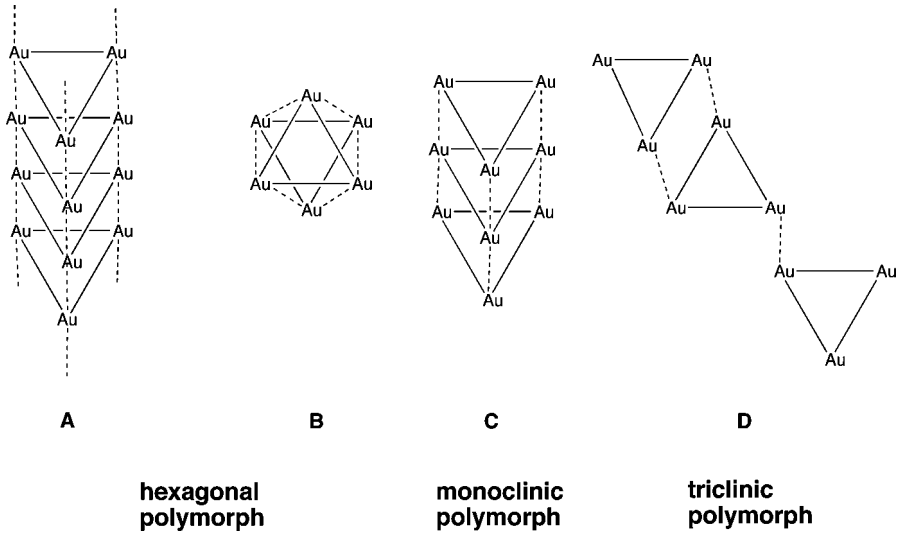

tions compete with other forces in the solid state to produce the observed structures.

In the hexagonal form of $Au_3(MeN{=}COMe)_3$, which is the only form to display solvoluminescence, the trimers form two types of stacks, **A** and **B** in Chart 2.[2] One stack (**A**) is prismatic with close Au···Au contacts of 3.346(1) Å between molecules. The other type of stack (**B**) is disordered with two positions for the triangles of gold atoms that are offset by 60°. The monoclinic polymorph contains short prismatic stacks that consist of only three of the trinuclear molecules with an out-of-plane Au···Au distance of 3.28(3) Å.[4] The triclinic polymorph does not contain any sort of stacks but does have two different types of Au···Au interactions between the trimers.[4] The hexagonal form is the only polymorph that has extended, linear chains of gold(I) ions.

Previously, it was suggested that the long-lived emission from the hexagonal form of $Au_3(MeN{=}COMe)_3$ resulted from charge separation that was facilitated by the mobility of electrons along the extended chains of gold(I) ions, which are uniquely present in this particular polymorph.[2] Consequently, it is important to understand the various redox reactions that $Au_3(MeN{=}COMe)_3$ might undergo. Chemical oxidation of $Au_3(MeN{=}COMe)_3$ with molecular iodine or bromine produced the series of complexes $Au_3X_n(MeN{=}COMe)_3$ (where n could be 2, 4, or 6). In these complexes, the two-coordinate gold(I) ions were successively oxidized to four-coordinate gold(III) centers.[1,8] Upon exposure to solutions of electron acceptors such as various nitrofluorenones, $Au_3(MeN{=}COMe)_3$ forms charge-transfer adducts.[9] For example, crystals of deep-yellow $Au_3(MeN{=}COMe)_3$·2,4,7-trinitro-9-fluorenone and red $Au_3(MeN{=}COMe)_3$·2,4,5,7-tetranitro-9-fluorenone, in which the planar donors and acceptors are interleaved, have been isolated and characterized by single crystal X-ray diffraction.

Electrically conducting molecular salts may be formed by the process of electrocrystallization, which generally involves oxidation of an appropriate metal complex in solution at an electrode surface.[10] Crystals of a number of partially (or factionally) oxidized complexes of platinum (e.g. $K_{1.74}Pt(CN)_4$, $KPt(CN)_4Cl_{0.3}$, $K_{1.64}Pt(O_2C_2O_2)_2$)[10−12] and iridium (e.g. $(Et_4N)_{0.55}Ir(CO)_2Cl_2$)[13]) have been obtained through electrochemical oxidation of solutions of the appropriate Pt(II) or Ir(I) complex. It is also possible to obtain these materials through chemical oxidation. These partially oxidized complexes generally crystallize as needles that have a metallic golden color.[10] Structurally, they consist of extended stacks of the planar metal ions connected by short metal−metal bonds. The partially oxidized salts conduct electricity anisotropically with high conductivity along the direction of the needle, which is also the direction of the stacking, and insulating character in the perpendicular directions. Additionally, metal−metal bonded polymers having the general formula $\{M(bpy)(CO)_2\}_n$ (M = Ru and Os) have been obtained from electrocrystallization beginning with *trans*-(Cl)-$[Ru(bpy)(CO)_2Cl_2]$ and its osmium analogue.[14] Another metal chain polymer, $\{[Rh_4(\mu\text{-}OOCCH_3)_4(phen)_4]^{2+}\}_n$, has also been obtained through electrocrystallization.[15]

Here, we present results of a study of the electrochemical behavior of $Au_3(MeN{=}COMe)_3$ in solution.

Results

Electrochemical oxidation of $Au_3(MeN{=}COMe)_3$ in dichloromethane solution with 0.10 M tetra(*n*-butyl)am-

(8) Vickery, J. C.; Balch, A. L. *Inorg. Chem.* **1997**, *36*, 5978.
(9) Olmstead, M. M.; Jiang, F.; Attar, S.; Balch, A. L. *J. Am. Chem. Soc.* **2001**, *123*, 3260.
(10) Miller, J. S. *Science* **1976**, *194*, 189.
(11) Williams, J. M.; Gerrity, D. P.; Schultz, A. J. *J. Am. Chem. Soc.* **1977**, *99*, 1668.
(12) Xu, L.; Dong, S. *Electrochim. Acta* **1994**, *29*, 2599.
(13) Wysocka, M.; Winkler, K.; Stork, J. R.; Balch, A. L. *Chem. Mater.* **2004**, *16*, 771.
(14) (a) Hartl, F.; Mahabiersing, T.; Chardon-Noblat, S.; Da Costa, P.; Deronzier, A. *Inorg. Chem.* **2004**, *43*, 7250. (b) Chardon-Noblat, S.; Cripps, G. H.; Deronzier, A.; Fields, J. S.; Gauws, S.; Haines, R. J.; Southwany, F. *Organometallics* **2001**, *20*, 1668. (c) Chardon-Noblat, S.; Deronzier, A.; Hartl, E.; Von Slageren, J.; Mahabiersing, T. *Eur. J. Inorg. Chem.* **2001**, 613.
(15) Lafolet, F.; Chardon-Noblat, S.; Duboc, C.; Deronzier, A.; Pruchnik, F. P.; Rak, M. *Dalton Trans.* **2008**, 2149.

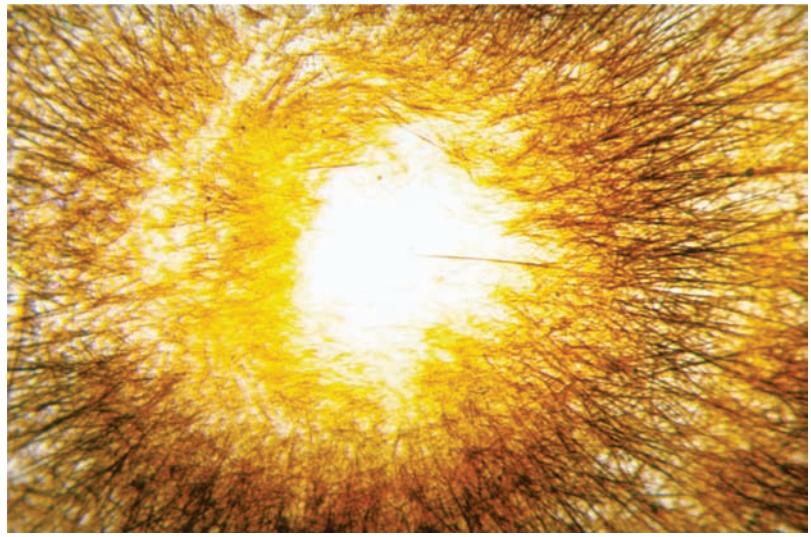

Figure 1. A photograph of the crystals formed by oxidation of $Au_3(MeN{=}COMe)_3$ at a constant potential of +650 mV in a dichloromethane solution containing 0.10 M tetra(*n*-butyl)ammonium perchlorate. The electrode, which had a diameter of 1.5 mm, was removed from the solution and created the open space in the center of the crystalline deposit.

monium perchlorate as supporting electrolyte at +650 mV was accompanied by the growth of fine, needle-like crystals that radiate outward from the electrode. Figure 1 shows a photograph of the shiny, golden needles that were left as a pad in the electrolysis solution after the electrode was removed. The crystals produced in this fashion were extremely thin and none were found that were suitable for single crystal X-ray diffraction. Consequently, a more detailed electrochemical study of the oxidation process was undertaken. A similar attempt to oxidize $Au_3(PhCH_2N{=}COMe)_3$ did not result in the deposition of any crystalline (or noncrystalline) material.

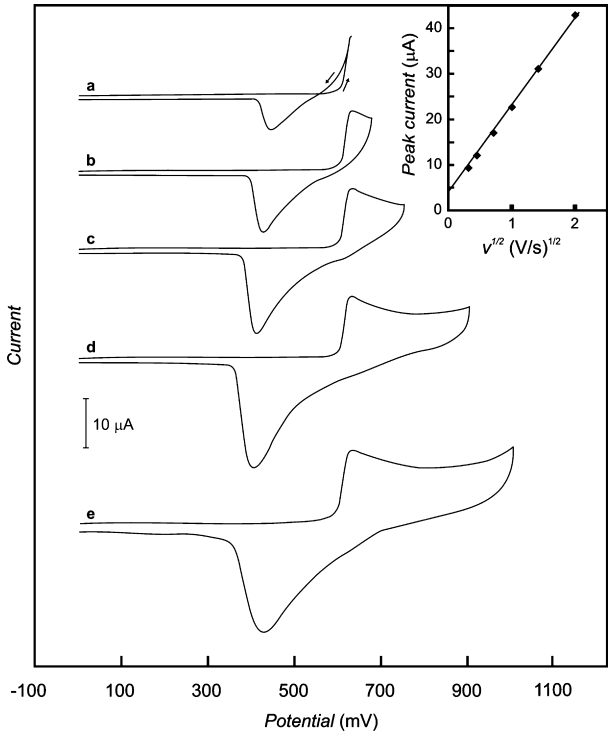

Figure 2. Cyclic voltammograms recorded for a 1.0 mM solution of $Au_3(MeN{=}COMe)_3$ in dichloromethane containing 0.10 M tetra(*n*-butyl)ammonium perchlorate at a gold electrode (1.5 mm diameter) in the potential range (a) 0 to 600 mV, (b) 0 to 700 mV, (c) 0 to 800 mV, (d) 0 to 900 mV, and (e) 0 to 1000 mV. The sweep rate was 100 mV s^{-1}. The inset shows dependence of the oxidation peak current on the square root of sweep rate.

Cyclic Voltammetric and Morphological Studies of the Oxidation of $Au_3(MeN{=}COMe)_3$. Cyclic voltammetric curves recorded for a dichloromethane solution of $Au_3(CH_3N{=}COCH_3)_3$ containing tetra(*n*-butyl)ammonium perchlorate as supporting electrolyte are shown in Figure 2. These curves exhibit shapes that are indicative of the process of electrocrystallization. In the anodic cycle, the current for oxidation of the gold trimer increased sharply after a potential of 550 mV was reached. The peak potential for the oxidation process occurred at 630 mV. The reduction peak at 420 mV that was associated with this reduction exhibited behavior typical of a process involving a surface confined species. The ratio of the charge transferred upon reduction to the charge transferred upon oxidation was close to 1. The anodic peak current depended linearly on the square root of the sweep rate with a positive intercept on the current axis as seen in the inset in Figure 2. Such features are commonly observed for electrode processes that are controlled by nucleation.[16]

Similar voltammetric experiments were performed in dichloromethane solution containing different supporting electrolytes. With variation of the anion, shifts of the oxidation potential toward more positive values were observed in the order: $(BF_4)^-$, 582 mV < $(PF_6)^-$, 615 mV < $(ClO_4)^-$, 630 mV. No effect was observed on the potential for oxidation from changing the cation in supporting electrolyte. For all supporting electrolytes that were examined, the ratio of charge for reduction to charge for oxidation was close to 1.

The morphologies of the deposits formed by oxidation of $Au_3(MeN{=}COMe)_3$ on a gold electrode are shown in Figure 3. Crystals were produced under potentiostatic conditions with different oxidation times. For short deposition times,

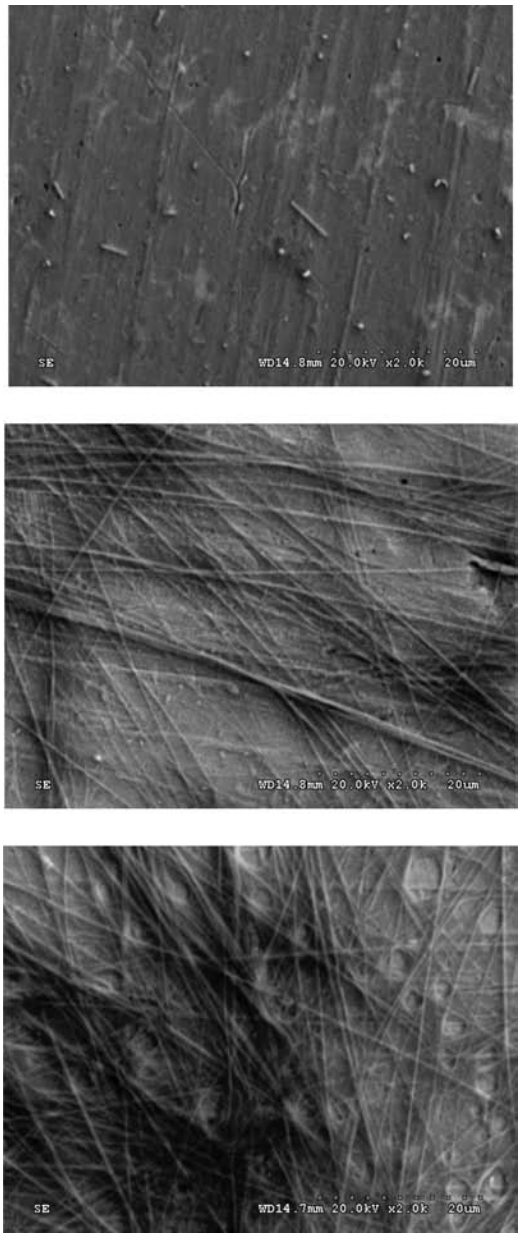

Figure 3. SEM images of the 1D crystals formed on the surface of gold foils during potentiostatic oxidation of 1.0 mM solution of $Au_3(MeN{=}COMe)_3$ in dichloromethane containing 0.10 M tetra(*n*-butyl)ammonium perchlorate at a potential of +650 mV. The time of electrolysis was (a) 15 s, (b) 30 s, and (c) 90 s.

Table 1. Size of Crystals Formed on the Electrode Surface under Potentiostaic Conditions at +650 mV in Dichloromethane Containing 0.1 M Tetra(*n*-butyl)ammonium Perchlorate

		crystal size	
$[Au_3(MeN{=}COMe)_3$ concentration (mM)	time (s)	Length (μm)	Width (nm)
1.0	15	2–4	~50
	30	30–40	~80
	60	80–100	~100
	90	130–160	~110
2.0	15	30–50	~60
	30	110–130	~100

small crystals (as indicated by the arrows in part a of Figure 3) were observed on the electrode surface. Because there was a large distribution in the sizes of these crystals, it is likely that progressive nucleation occurred during oxidation.

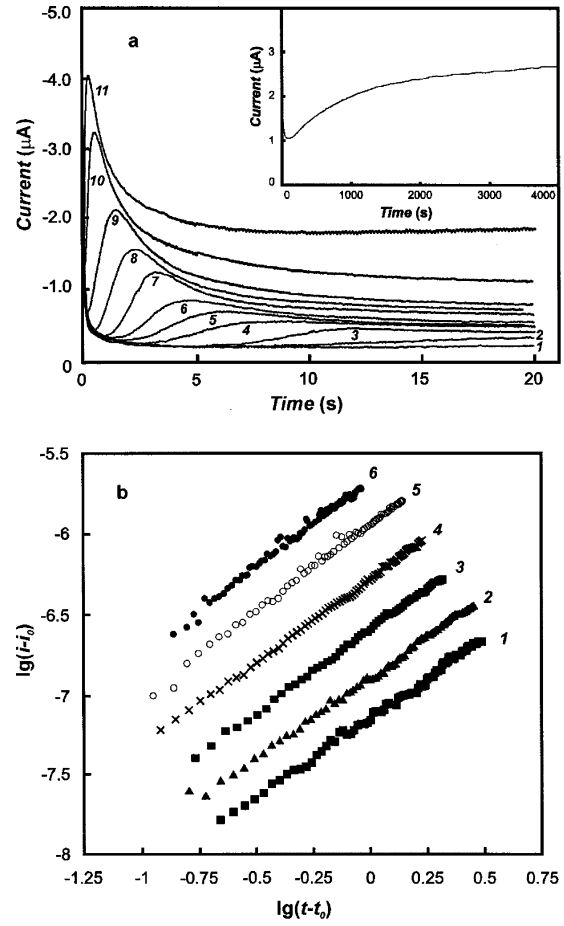

Figure 4. (a) Chronoamperometric curves of the oxidation recorded in dichloromethane containing 1.1 mM $Au_3(MeN{=}COMe)_3$ and 0.10 M tetra(*n*-butyl)ammonium perchlorate at a gold electrode (1.5 mm diameter) at (*1*) 500 mV, (*2*) 535 mV, (*3*) 542 mV, (*4*) 550 mV, (*5*) 558 mV, (*6*) 566 mV, (*7*) 574 mV, (*8*) 582 mV, (*9*) 590 mV, (*10*) 598 mV, and (*11*) 606 mV. The inset shows the dependence of the current on the time under potentiostatic oxidation at +650 mV. (b) Double logarithmic analyses of the rising parts of the current−time transients obtained for (*1*) 550 mV, (*2*) 558 mV, (*3*) 566 mV, (*4*) 574 mV, (*5*) 590 mV, and (*6*) 598 mV.

Subsequently, the crystals grew more rapidly. After 30 s of oxidation, long, thin needles (about 50−80 μm long and 50−70 nm thick) were formed on the electrode surface as seen in part b of Figure 3. Upon lengthier electrocrystallization, long crystallites grew on the electrode surface as seen in part c of Figure 3 and in Figure 1. These long, golden needles grew outwardly and perpendicularly to the electrode surface. The deposit formed a brushlike structure on the electrode surface. Table 1 gives the sizes of needles that are formed at different electrolysis times.

Chronoamperometric Studies of Crystal Growth from $Au_3(MeN{=}COMe)_3$. The growth of the 1D crystals on the electrode surface was probed by chronoamperometry. Part a of Figure 4 shows the current (i) versus time (t) transients obtained for the oxidation of $Au_3(MeN{=}COMe)_3$ at different potentials. These curves exhibited features characteristic of nucleation and growth of a new phase on the electrode surface.[17] The initial decay of the oxidation current to a minimum value (i_o) was followed by a rising transient due to the formation and subsequent growth of nuclei of the new phase. After reaching a maximum value, the current subse-

quently decreased slowly with time. Plots of ln i versus ln t for the rising parts of the current−time transients produced excellent straight lines with slopes of 1.05 ± 0.07 as seen in part b of Figure 4. A linear ln i versus ln t relationship with a slope equal to unity is predicted for progressive nucleation followed by 1D growth of needle-like microcrystals.[16] In this case, the $i-t$ relationship is expressed by the following equation:[16]

$$i-i_o = nFAL^2k(t-t_o) \quad (1)$$

where F is the Faradaic constant, t_o is the time to reach the current minimum value (i_o), n is the number of electrons exchanged, A is nucleation rate constant, k is the rate constant for the crystal growth, and L is the rate of formation of the nuclei.

At times longer than about 50 min, the current approached a limiting value. Such behavior was related to a significance increase in the electrode area. This behavior also indicated that the new phase that grew on the electrode surface was conductive.

Stoichiometry of the Oxidative Process. The formation of 1D crystals by partial oxidation of $Au_3(MeN{=}COMe)_3$ can be described by the following equation:

$$[Au_3(MeN{=}COMe)_3 + xClO_{4^-} \rightleftarrows [Au_3(MeN{=}COMe)_3](ClO_4)_x + xe^- \quad (2)$$

The results of the voltammetric study showed that the yield of the electrocrystallization process was close to 100%. The electrochemical behavior indicated that the crystals that formed on the electrode surface were conductive. Under these conditions, bulk electrolysis can be used for determination of the number of electrons exchanged, x, during the oxidation process and the stoichiometry of electro-deposited crystals.

Part a of Figure 5 shows current versus time transients for the bulk electrolysis of $Au_3(MeN{=}COMe)_3$ at a potential of +650 mV carried out in solutions with two different concentrations of the gold trimer. At long times, the current approached a limiting value, indicating complete oxidation of the trimer. Part b of Figure 5 shows the linear relation between the oxidation charge, Q_{ox}, obtained by the integration of the current versus time transients, and concentration of the trimer in solution. Such a relation is predicted by the Faraday law. From the slope of this relation, the number of electrons exchanged during oxidation, x, was found to be 0.35. The concentration of reactant in the electrolyzed solution was monitored using cyclic voltammetry as shown in part c of Figure 5. After 100 min of prolonged electrolysis, the peak for $[Au_3(MeN{=}COMe)_3$ oxidation disappeared indicating complete oxidation of the trimer during electrolysis.

The number of electrons exchanged during the oxidation process can be also determined using an electrochemical quartz crystal microbalance (EQCM) technique. This method

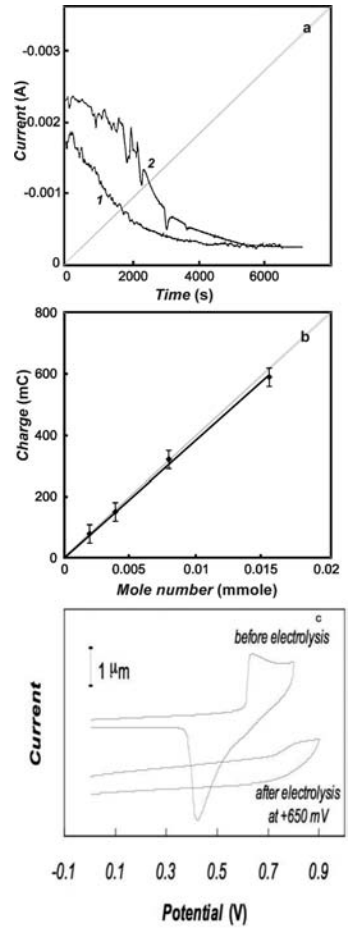

Figure 5. (a) Current−time transients recorded during potentiostatic electrolysis at +650 mV in a solution of (*1*) 1.0 mM $Au_3(MeN{=}COMe)_3$ and 0.10 M tetra(*n*-butyl)ammonium perchlorate and (*2*) 2.0 mM $Au_3(MeN{=}COMe)_3$. (b) Dependence of total oxidation charge on the molar concentration of $Au_3(MeN{=}COMe)_3$ in solution. (c) Cyclic voltammograms run before and after electrolysis at 650 mV.

was described in a previous paper.[18] The results of EQCM studies of the oxidation of $Au_3(MeN{=}COMe)_3$ in dichloromethane solution containing tetra(*n*-butyl)ammonium perchlorate are shown in Figure 6. On the basis of the mass changes (Δm) and the charge (Q_R) for reduction of the 1D crystals, the value of x can be calculated for eq 2. In this case the following equation was used:[18]

$$\Delta m = \frac{xM_{ClO_4^-} + M_{[Au_3(MeN{=}COMe)_3]}}{xF} Q_R \quad (3)$$

The value of Δm was calculated from the frequency changes of the quartz crystal during 1D crystal reduction. Q_R was calculated by integration of the voltammetric peak current for the reduction of the crystals. On the basis of eq 3, a value of x of 0.33 was calculated for the $[Au_3(MeN{=}COMe)_3](ClO_4)_x$ salt. This value is in agreement with coefficient x obtained on the basis of bulk electrolysis as described above.

X-ray Powder Diffraction Studies. Because crystals suitable for single crystal X-ray diffraction were not avail-

(16) Guanawardena, G.; Hills, G.; Montenegro, I. *J. Electroanal. Chem.* **1985**, *184*, 371.
(17) Harrison, J. A.; Thirsk, H. R. In *Electroanalytical Chemistry*; Bard, A. J., Ed.; Marcel Dekker: New York, 1971; Vol. *5*, p 67.
(18) Winkler, K.; Wysocka-Zolopa, M.; Olesicka, M. M.; Recko, K.; Dobrzynski, L.; Stork, J. R.; Gussenhoven, E. M.; Olmstead, M. M.; Balch, A. L. *Electrochim. Acta* **2008**, *53*, 7288.

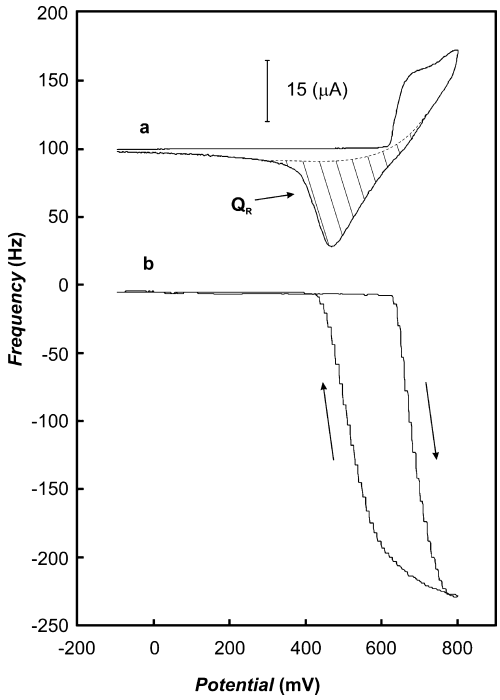

Figure 6. Voltammograms and curves of frequency change vs potential simultaneously recorded at the same Au/quartz electrode in a dichloromethane solution containing 1.0 mM $Au_3(MeN{=}COMe)_3$ and 0.10 M tetra(*n*-butyl)ammonium perchlorate. The sweep rate was 25 mV s^{-1}.

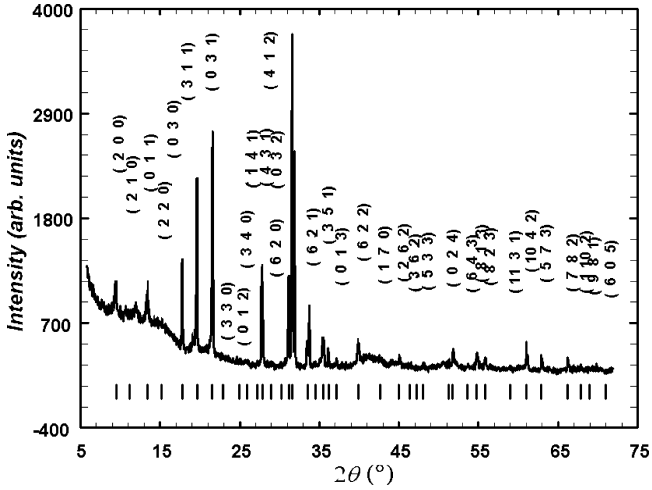

Figure 7. XRD diagrams collected at RT using Fe Kα radiation for the product of electro-oxidation of $Au_3(MeN{=}COMe)_3$ at +620 mV in dichloromethane containing 0.10 M tetra(*n*-butyl)ammonium perchlorate.

able, the crystallites produced by electro-oxidation were examined by powder X-ray diffraction at room temperature using Fe Kα radiation. Figure 7 shows the powder diffraction data obtained from the electro-oxidized sample. The data were analyzed by means of the Rietveld-type *FULLPROF* program[19] and indexed to the orthorhombic space group *Pmmm* with $a = 23.49(3)$, $b = 19.48(2)$, and $c = 9.17(2)$ Å. The diffraction pattern observed for the oxidized was clearly distinct from those of the hexagonal, triclinic, and monoclinic polymorphs of the precursor, $Au_3(MeN{=}COMe)_3$, and confirmed the crystalline nature of the material.

Cyclic Voltammetry for $Au_3(PhCH_2N{=}COMe)_3$. Figure 8 shows cyclic voltammograms from a solution of

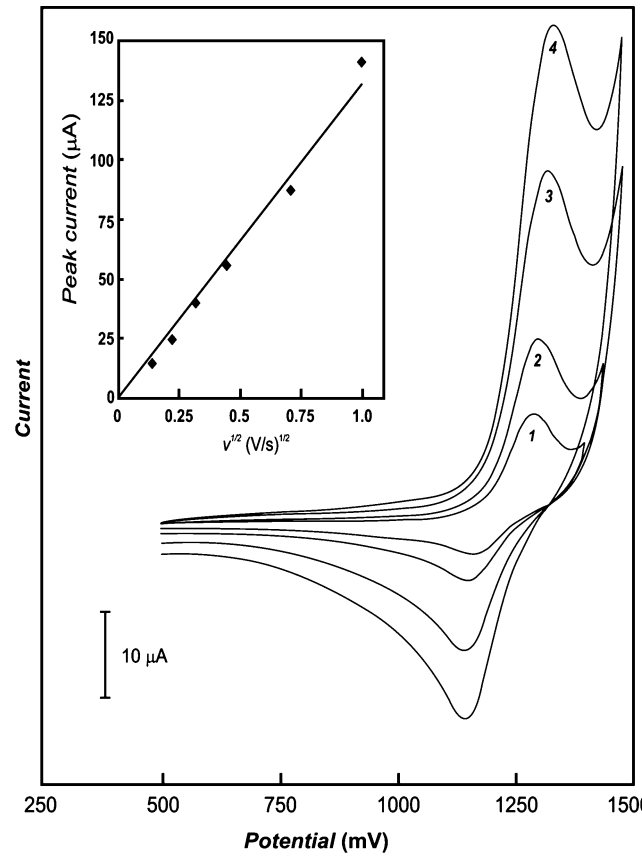

Figure 8. Cyclic voltammograms recorded in dichloromethane containing 1.08 mM $Au_3(PhCH_2N{=}COMe)_3$ and 0.10 M tetra(*n*-butyl)ammonium perchlorate at an Au (1.5 mm diameter) electrode. Sweep rate was (*1*) 20 mV s^{-1}, (*2*) 50 mV s^{-1}, (*3*) 100 mV s^{-1}, and (*4*) 200 mV s^{-1}. The inset shows dependence of the oxidation peak current on the square root of sweep rate.

$Au_3(PhCH_2N{=}COMe)_3$[20] in dichloromethane containing tetra(*n*-butyl)ammonium perchlorate at different sweep rates. The cyclic voltammograms are characteristic of a diffusion-controlled process. Notice that the potential for oxidation is shifted significantly in a positive direction in comparison to the oxidation peak observed for $Au_3(MeN{=}COMe)_3$. The current of the oxidation peak depended linearly on the square root of the sweep rate with an intercept equal to zero. However, the ratio of cathodic to anodic peak current was less than 1. This behavior indicated that the electro-oxidation of $Au_3(PhCH_2N{=}COMe)_3$ was followed by an additional process that led to the decomposition of the oxidized product. In contrast to the situation for $Au_3(MeN{=}COMe)_3$, no deposit was observed on the electrode surface after prolonged electrolysis of $Au_3(PhCH_2N{=}COMe)_3$ at constant potential.

Discussion

During electro-oxidation of $Au_3(MeN{=}COMe)_3$ in dichloromethane solution, needle-like crystals were deposited on the electrode surface. The electrochemical process in the presence of perchlorate anion can be described by the following equation:

(19) Rodriguez-Carvajal, J. *Phys. B* **1993**, *192*, 55.

(20) Balch, A. L.; Olmstead, M. M.; Vickery, J. C. *Inorg. Chem.* **1999**, *38*, 3494.

$$[Au_3(MeN{=}COMe)_3] + 0.34\ ClO_{4^-} \rightleftharpoons [Au_3(MeN{=}COMe)_3](ClO_4)_{0.34} + 0.34\ e^- \quad (4)$$

The composition of the needles has been determined by both bulk electrolysis and quartz crystal microbalance techniques. Both methods agree that the composition of the product is $[Au_3(MeN{=}COMe)_3](ClO_4)_{0.34}$. Within limits, the size of the needles deposited on the electrode surface was controlled by the rate of electrolysis (applied potential), the electrolysis time, and the concentration of complex in the solution. The increase of the current at the electrode covered with needle-like material indicated that the deposit was conductive.

The electrochemical behavior of $Au_3(MeN{=}COMe)_3$ and $Au_3(PhCH_2N{=}COMe)_3$ are noticeably different. Whereas $Au_3(MeN{=}COMe)_3$ forms crystalline $[Au_3(MeN{=}COMe)_3](ClO_4)_{0.34}$. $Au_3(PhCH_2N{=}COMe)_3$ undergoes oxidation at a more positive potential without the formation of a solid product. We attribute the different behaviors to differences in solubility of the oxidized product and steric effects of the benzyl group which inhibit stacking of molecules of $Au_3(PhCH_2N{=}COMe)_3$.

The chemical behaviors of four-coordinate d^8 and two-coordinate d^{10} metal complexes show a number of important parallels with regard to the nature of the metal−metal interactions that can occur. Both types of complexes have a tendency to self-associate through attractive, metallophilic interactions.[21] These interactions lead to the formation of extended chains of the metal complexes with relatively short distances between the metal ions. Relevant examples include the numerous salts of $[Pt(CN)_4]^{2-}$[22] and $[Au(CN)_2]^-$.[23−25] Oxidative additions to certain four-coordinate d^8 complexes produce dinuclear d^7 complexes with direct metal−metal bonding.[26] Likewise, there are Au(I) complexes that undergo oxidative addition to form dinuclear d^9 complexes with direct Au−Au single bonds.[27,28] A number of partially oxidized salts of platinum and iridium have been prepared by chemical and electrochemical oxidation of Pt(II) (as well as Ir(I)) complexes.[9−13] These partially oxidized materials also contain stacks of the metal complexes with direct metal−metal bonding. In general, partial oxidation results in a shortening of the metal−metal separation in the oxidized product. However, to our knowledge, similar partially oxidized, extended linear chain gold complexes have not previously been described. For example, there have been numerous electrochemical examinations of salts of $[Au(CN)_2]^-$, which is widely used in electroplating, yet none of these mention the formation of any sort of partially oxidized material that would be analogous to $K_{1.74}Pt(CN)_4$ and $KPt(CN)_4Cl_{0.3}$.[29,30] Thus, $[Au_3(MeN{=}COMe)_3](ClO_4)_{0.34}$ appears to be the first example of a partially oxidized gold complex. However, there are examples of complexes containing finite, linear chains of five or six gold centers (e.g. $[Au_5]^{9+}$ and $[Au_6]^{10+}$) with fractional oxidation states.[31,32]

Finally, we speculate that the structure of the partially oxidized $[Au_3(MeN{=}COMe)_3](ClO_4)_{0.34}$ consists of stacks of the trimeric gold complex that are similar to those found in the hexagonal polymorph of $Au_3(MeN{=}COMe)_3$ itself. The observation that oxidation of $Au_3(MeN{=}COMe)_3$ forms a conducting solid, $[Au_3(MeN{=}COMe)_3](ClO_4)_{0.34}$, offers further insight into our suggestion that solvoluminescence involves energy storage involving electron mobility along chains of gold complexes.

Experimental Section

Materials. $Au_3(MeN{=}COMe)_3$ and $Au_3(PhCH_2N{=}COMe)_3$ were synthesized according to methods described in the literature.[1,7] The supporting electrolytes: tetra(*n*-butyl)ammonium perchlorate, (Fluka) tetra(*n*-butyl)ammonium tetrafluoroborate (Sigma Chemical Co.), and tetra(*n*-butyl)ammonium hexafluorophosphate (Sigma Chemical Co.) were dried under vacuum for 24 h prior to use. Dichloromethane was used as received from Aldrich.

Instrumentation. Standard voltammetric experiments were performed on potentiostat/galvanostat Model 283 (EG&G Instruments) with a three-electrode cell. A gold disk electrode with a diameter of 1.5 mm (Bioanalytical Systems Inc.) was used as the working electrode. Prior to each experiment, the electrodes were polished with fine carborundum paper and then with a 0.5 μm alumina slurry. Subsequently, the electrodes were sonicated in water to remove the traces of alumina from the gold surface, washed with water, and dried. In bulk electrolyses, a platinum foil with a surface area of about 1 cm^2 served as the working electrode. A silver wire immersed in 0.010 M silver nitrate and 0.09 M tetra(*n*-butyl)ammonium perchlorate in acetonitrile was separated from the working electrode by a ceramic tip (Bioanalytical Systems Inc.) and served as the reference electrode. With this reference electrode, the ferrocene/ferrocenium formal redox potential was +204 mV. The counter electrode was a platinum tab with an area of about 0.5 cm^2. In large-scale electrolyses, this electrode was separated from the solution by a glass frit.

Simultaneous voltammetric and piezoelectric microgravimetry experiments were carried out with a home-built potentiostat and electrochemical quartz crystal microbalance, EQCM 5510, from the Institute of Physical Chemistry (Warsaw, Poland). Because plano-convex quartz crystals confine acoustic energy to the center of the crystal much better than the plano-plano crystals, the former were used. The 14 mm diameter AT-cut, plano-convex quartz crystals with 5 MHz resonant frequencies were obtained from Omig (Warsaw, Poland). A 100 nm gold film, which was vacuum deposited on the quartz crystal, served as the working electrode. The area of this gold electrode, which included a 5 mm in diameter

(21) Pyykkö, P. *Chem. Rev.* **1997**, *97*, 597.
(22) Williams, J. M. In *Extended Linear Chain Compounds*; Miller J. S., Ed.; Plenum: New York, 1982; Vol. *1*, p 73.
(23) Rawashdeh-Omary, M. A.; Omary, M. A.; Patterson, H. H.; Fackler, J. P., Jr. *J. Am. Chem. Soc.* **2001**, *123*, 11237.
(24) (a) Leznoff, D. B.; Xue, B.-Y.; Batchelor, R. J.; Einstein, F. W. B.; Patrick, B. O. *Inorg. Chem.* **2001**, *40*, 6026. (b) Shorrock, C. J.; Xue, B.-Y.; Kim, P. B.; Batchelor, R. J.; Patrick, B. O.; Leznoff, D. B. *Inorg. Chem.* **2002**, *41*, 6743.
(25) (a) Stender, M.; Olmstead, M. M.; Balch, A. L.; Rios, D.; Attar, S. *Dalton Trans.* **2003**, 4282. (b) Pham, D. M.; Rios, D.; Olmstead, M. M.; Balch, A. L. *Inorg. Chim. Acta* **2005**, *358*, 4261–4269.
(26) Che, C. M.; Schaefer, W. P.; Gray, H. B.; Dickson, M. K.; Stein, P. B.; Roundhill, D. M. *J. Am. Chem. Soc.* **1982**, *104*, 4253.
(27) Fackler, J. P., Jr.; Basil, J. D. *Organometallics* **1982**, *1*, 871.
(28) Mazany, A. M.; Fackler, J. P., Jr. *J. Am. Chem. Soc.* **1984**, *106*, 801.
(29) Eisenmann, E. T. *J. Electrochem. Soc.* **1978**, *125*, 717.
(30) Harrison, J. A.; Thompson, J. *J. Electroanal. Chem.* **1972**, *40*, 113.
(31) Usón, R.; Laguna, A.; Laguna, M.; Jiménez, J.; Jones, P. G. *Angew. Chem., Int. Ed. Engl.* **1991**, *30*, 198.
(32) Laguna, A.; Laguna, M.; Jiménez, J.; lahoz, F. J.; Olmos, E. *Organometallics* **1994**, *13*, 253.

circuit center spot and two contacting radial strips, was 0.24 cm^2. Unpolished quartz crystals were used for better adherence of the film. The sensitivity of the mass measurement, as calculated from the Saurbrey equation, was 17.7 ng Hz^{1-} cm^{-2}

Scanning electron micrograph (SEM) images were obtained with the use of a LEO 435 vp microscope. The acceleration voltage of the electron beam was 7 kV. Samples for SEM studies were prepared by constant potential electro-deposition on a gold foil. The electrodes covered with gold crystals were rinsed with dichloromethane and then placed under the microscope.

X-ray powder diffraction (XRD) measurements carried out on a two axis HZG-4C diffractometer. The patterns were obtained with Fe Kα radiation ($\lambda = 1.93597$ Å) and Mn β-filter at a tube voltage of 25 kV and a tube current of 20 mA.

Acknowledgment. We thank the State Committee for Scientific Research, Poland (project No. 3T09A 167 28 to KW) and the United States National Science Foundation (Grants CHE-0716843 and CHE-0413857 to ALB) for financial support, and S. Wojtulewski for assistance with the preparation of the figures.

IC801922A